

IPMSM Model Including Magnetic Saturation and Cross-Coupling

Darko P. Marčetić, Roberto M. Varga, and Mile B. Božić

Abstract—This paper presents a modified IPMSM model suitable for use with carrier-signal-injection-based sensorless methods. The suggested model includes magnet saturation of both d- and q- axis and cross-coupling which all result in more accurate description of high frequency test signal propagation. The model is verified by comparing experimental results of a sensorless method based on HF test signal with simulation results from standard and modified model.

Index Terms—IPMSM, model, HF test signal sensorless.

NOMENCLATURE

| | |
|------------------------|---|
| v_d, v_q | – stator d - and q - axis voltages |
| i_d, i_q | – stator d - and q - axis currents |
| v_{dh}, v_{qh} | – stator d - and q - axis high frequency voltage components |
| i_{dh}, i_{qh} | – stator d - and q - axis high frequency current components |
| ψ_d, ψ_q | – stator d - and q - axis fluxes |
| ψ_f | – permanent magnet flux |
| R_s | – stator phase resistance |
| L_d, L_q | – stator d - and q - axis self inductances |
| L_{dh}, L_{qh} | – stator d - and q - axis incremental self inductances |
| L_{dqh}, L_{qdh} | – stator d - and q - axis incremental mutual inductances |
| θ_r, θ_r^e | – actual and estimated rotor electrical position |
| ω_r | – actual rotor electrical angular frequency |
| T_e | – electromagnetic torque |
| P | – number of pole pairs |

I. INTRODUCTION

INTERIOR Permanent Magnet Synchronous Machine (IPMSM) is used in many motor drive applications mostly due to its cost, high efficiency and high torque-to-inertia ratio [1]. Further drive system cost reduction is only possible if shaft position sensor is eliminated. The most popular methods for IPMSM rotor position estimation are a carrier-signal-injection-based methods. Those methods bypass fundamental

Manuscript received 30 May 2012. Accepted for publication 10 June 2012. Some results of this paper were presented at the 16th International Symposium Power Electronics, Novi Sad, Serbia, October 26-28, 2012.

This work was supported by Ministry of Education and Science of the Republic Serbia within project III 42004.

D. Marčetić is with the Faculty of Faculty of Technical Sciences, University of Novi Sad, , Serbia:(phone: +381-21-485-2504; e-mail: darmar@uns.ac.rs).

R. Varga is with Neotech Ltd, Novi Sad, Serbia (e-mail: neotech@open.telekom.rs).

M. Božić is with Nidec Motor Corporation, Chicago, USA (e-mail: mile.bozic@nidec-motor.com).

BEMF limitations by injecting a HF voltage signal into the phase windings and by measuring the machine response detecting corresponding HF current. The HF signal can be injected as rotating carrier in the stationary reference frame [2], [3] or as pulsating signal into the estimated d-axis [4], [5]. Usage of test signal injection helps but does not fully cancel the methods dependence on motor parameters variation. It has been reported that both saturation and cross-coupling effects introduce load dependent rotor position error [6] – [10].

This paper presents improved IPMSM model that helps explaining motor load dependence of HF test signal based methods. The model includes magnet saturation of both d- and q- axis and cross-coupling magnetic saturation. Experimental results show that only suggested model modifications bring model results close to experimental results under the heavy loading conditions.

II. MATHEMATICAL MODEL OF IPMSM WITH AND WITHOUT SATURATION AND CROSS-COUPLING

Electrical subsystem of IPMSM can be modeled using voltage balance equations (1), flux linkage equations (2) and electromagnetic torque formula (3).

$$\begin{bmatrix} v_d \\ v_q \end{bmatrix} = \begin{bmatrix} R_s & 0 \\ 0 & R_s \end{bmatrix} \begin{bmatrix} i_d \\ i_q \end{bmatrix} + \begin{bmatrix} p & -\omega_r \\ \omega_r & p \end{bmatrix} \begin{bmatrix} \psi_d \\ \psi_q \end{bmatrix} \quad (1)$$

$$\begin{bmatrix} \psi_d \\ \psi_q \end{bmatrix} = \begin{bmatrix} L_d & 0 \\ 0 & L_q \end{bmatrix} \begin{bmatrix} i_d \\ i_q \end{bmatrix} + \begin{bmatrix} \psi_f \\ 0 \end{bmatrix} \quad (2)$$

$$T_e = \frac{3}{2} P [\psi_f i_q + (L_q - L_d) i_d i_q] \quad (3)$$

The state space model of IPMSM is given in (4)

$$p \begin{bmatrix} i_d \\ i_q \end{bmatrix} = [A] \begin{bmatrix} i_d \\ i_q \end{bmatrix} + [B] \begin{bmatrix} v_d \\ v_q \\ \omega_r \psi_f \end{bmatrix} \quad (4)$$

where

$$[A] = \begin{bmatrix} -\frac{R_s}{L_d} & \frac{\omega_r L_q}{L_d} \\ -\frac{\omega_r L_d}{L_q} & -\frac{R_s}{L_q} \end{bmatrix} \quad [B] = \begin{bmatrix} \frac{1}{L_d} & 0 & 0 \\ 0 & \frac{1}{L_q} & -\frac{1}{L_q} \end{bmatrix}$$

This is basic model that does not include d- and q-axis magnetic saturation nor cross-coupling saturation. The magnet saturation can be included by altering L_d and L_q parameter with current level using following functions.

$$\begin{aligned} L_d &= L_d(i_d, i_q) \\ L_q &= L_q(i_d, i_q) \end{aligned} \quad (5)$$

L_d and L_q variation can be mapped for different current levels using finite-element analysis or experimental results. Experimental results for tested motor for $L_d(i_d, i_q)$ and $L_q(i_d, i_q)$ are given on the Fig 1 and Fig 2.

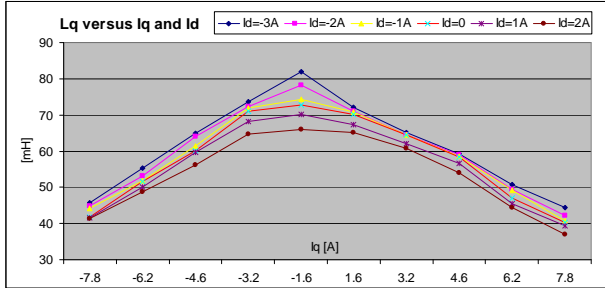


Fig. 1. Measured $L_q = L_q(i_d, i_q)$.

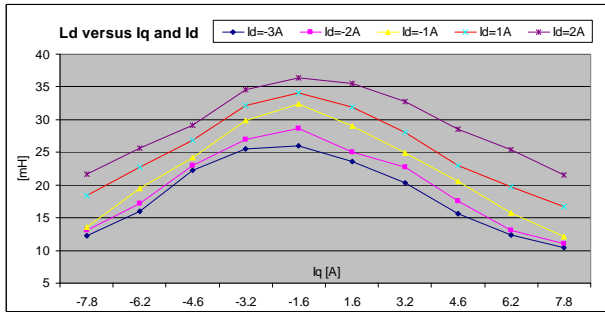


Fig. 2. Measured $L_d = L_d(i_d, i_q)$.

The cross coupling magnet saturation can be also built-in in IPMSM model using L_{dq} inductance parameter

$$\begin{bmatrix} \psi_d \\ \psi_q \end{bmatrix} = \begin{bmatrix} L_d & L_{dq} \\ L_{dq} & L_q \end{bmatrix} \begin{bmatrix} i_d \\ i_q \end{bmatrix} + \begin{bmatrix} \psi_f \\ 0 \end{bmatrix} \quad (6)$$

One way to include L_{dq} is to alter the state space IPMSM model as shown in (7) and on Fig 3.

$$\begin{bmatrix} \dot{i}_d \\ \dot{i}_q \end{bmatrix} = \frac{1}{p} \left(\begin{bmatrix} A \\ B \end{bmatrix} \begin{bmatrix} i_d \\ i_q \end{bmatrix} + \begin{bmatrix} v_d \\ v_q \\ \omega_r \psi_f \end{bmatrix} \right) + \begin{bmatrix} 0 & -L_{dq}/L_d \\ -L_{dq}/L_q & 0 \end{bmatrix} \begin{bmatrix} i_d \\ i_q \end{bmatrix} \quad (7)$$

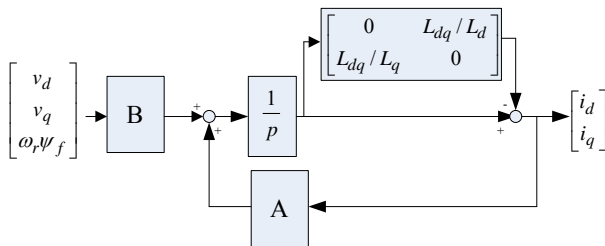


Fig. 3. Modified IPMSM model with build in cross-coupling saturation – suitable for MATLAB/ Simulink.

Cross coupling also changes with saturation and therefore L_{dq} parameter also has to vary with d- and q-axis current level. Measured $L_{dq} = L_{dq}(i_d, i_q)$ is given on the Fig 4. The data was collected experimentally, using approach suggested in [10].

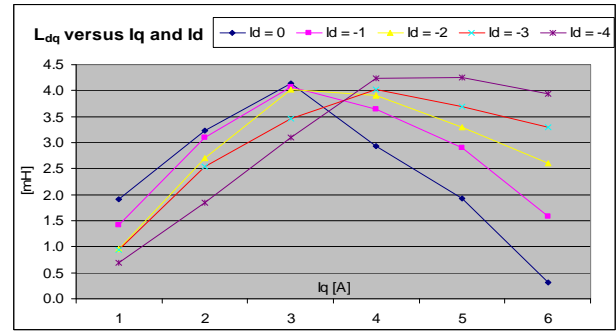


Fig. 4. Measured $L_{dq} = L_{dq}(i_d, i_q)$.

III. IPMSM MODEL EXCITED WITH INJECTED HF TEST SIGNAL AND UNDER DIFFERENT LOAD CONDITIONS

HF test signal based methods inject high frequency voltage signal into the phase windings and measure the machine response by detecting corresponding HF current signal. The HF q-axis current signal is compared to d-axis HF current signal and rotor position error signal is created, Fig 5.

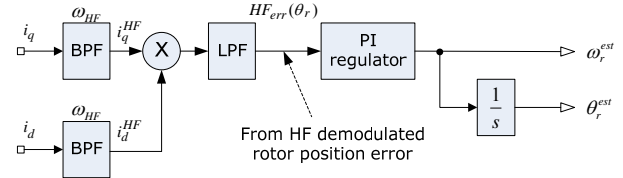


Fig. 5 The rotor position and speed estimation using demodulated HF current signal.

If only HF signals are considered, the model (1) and (6) reduces to

$$\begin{bmatrix} v_{dh} \\ v_{qh} \end{bmatrix} = \begin{bmatrix} L_{dh} & L_{dqh} \\ L_{qd} & L_{qh} \end{bmatrix} \cdot p \begin{bmatrix} i_{dh} \\ i_{qh} \end{bmatrix} \quad (8)$$

Equation (8) is valid in rotor position reference frame θ_r . However, the DSP can see only the quantities in used (estimated) rotor position reference frame, θ_r^e .

$$[T]^{-1} \begin{bmatrix} v_{dh}^e \\ v_{qh}^e \end{bmatrix} = \begin{bmatrix} L_{dh} & L_{dqh} \\ L_{qd} & L_{qh} \end{bmatrix} \cdot p [T]^{-1} \begin{bmatrix} i_{dh}^e \\ i_{qh}^e \end{bmatrix} \quad (9)$$

where $[T] = \begin{bmatrix} \cos(\theta_{err}) & \sin(\theta_{err}) \\ -\sin(\theta_{err}) & \cos(\theta_{err}) \end{bmatrix}$ transforms from θ_r to θ_r^e reference frame (Fig. 6).

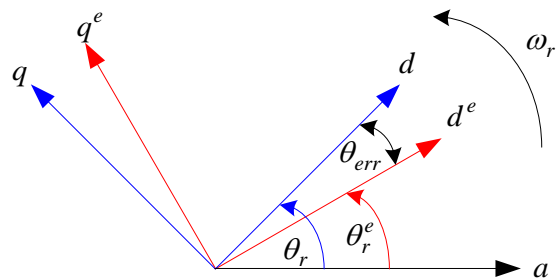


Fig. 6. Actual dq and estimated dq^e (DSP) rotating reference frames.

Therefore, if HF test signal v_{sig} is injected in d^e -axis only ($v_{dh}^e = v_{sig}$, $v_{qh}^e = 0$), in the estimated rotor position reference frame is valid (10)

$$\begin{bmatrix} v_{sig} \\ 0 \end{bmatrix} = \begin{bmatrix} L_{avg} - \hat{L}_{diff} \cos(2\theta_{err} + \theta_m) & \hat{L}_{diff} \sin(2\theta_{err} + \theta_m) \\ \hat{L}_{diff} \sin(2\theta_{err} + \theta_m) & L_{avg} + \hat{L}_{diff} \cos(2\theta_{err} + \theta_m) \end{bmatrix} p \begin{bmatrix} i_{dh}^e \\ i_{qh}^e \end{bmatrix}$$

where

$$L_{avg} = (L_{qh} + L_{dh})/2, L_{diff} = (L_{qh} - L_{dh})/2, \hat{L}_{diff} = \sqrt{L_{diff}^2 + L_{dq}^2}$$

$$\theta_m = \arctan(L_{dq} / L_{diff})$$

Solution of (10) for current d^e - and q^e -axis components available in DSP (estimated position reference frame) are

$$i_{dh}^e = \frac{v_{sig}}{p(L_{avg}^2 - \hat{L}_{diff}^2)} (L_{avg} + \hat{L}_{diff} \cos(2\theta_{err} + \theta_m)) \quad (11)$$

$$i_{qh}^e = -\frac{v_{sig}}{p(L_{avg}^2 - \hat{L}_{diff}^2)} (\hat{L}_{diff} \sin(2\theta_{err} + \theta_m))$$

Most of sensorless algorithms have estimated rotor position regulators that ultimately force i_{qh} signal to zero. If that is the case, according to (11) sensorless algorithm ends up with rotor position error equal to:

$$\theta_{err} = -\frac{\theta_m}{2} \quad (12)$$

Because of high dependence of relevant parameters (L_d , L_q and L_{dq}) of dc current levels in rotor position reference frame (Figures 1, 2, and 4) it is not easy to predict what will be the finally position error for giving load conditions. The only way to exam the nature of position error is to use modified simulation model which uses all inductance parameters as variables. Simulation results are given for no load $I_d = 0A$, $I_q = 0A$ (Fig. 7) and full load conditions $I_d = -4.5A$, $I_q = 5.5A$ (Fig. 8). The later pair is calculated using maximum torque per ampere approach. Both figures show trajectories of demodulated HF error signal (Fig 5.) for standard (dashed red) and for modified (solid blue) IPMSM model. Figures also show sawtooth signal of estimated rotor position which was artificially moved full circle around rotor position at stand still.

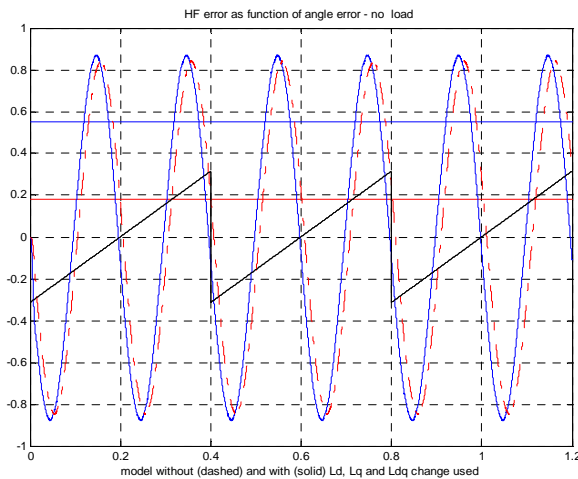


Fig. 7. Demodulated HF error signal as function of rotor position error for no load condition – model with (solid) and without (dashed) variable parameters.

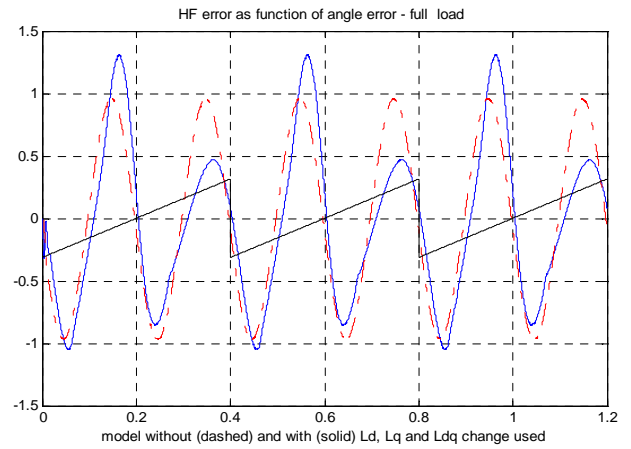


Fig. 8. Demodulated HF error signal as function of rotor position error for full load condition – model with (solid) and without (dashed) variable parameters.

Demodulated HF error signal holds position error information and drives sensorless position regulator. Standard IPMSM model predicts almost unchanged error signal trajectory for full circle of position error and therefore similar behavior of sensorless algorithm for different load conditions. On the other hand, modified IPMSM model predicts completely different nature of position error signal when load condition changes. Modified IPMSM model holds the reason for error signal deviation, the change is driven by significant L_d , L_q and L_{dq} inductance parameter variation with position error, as shown on Figure 9 for full load condition. While I_d^{DSP} and I_q^{DSP} for given load condition stay the same in DSP reference frame, the actual I_d and I_q vary with actual position error signal (in this case full circuit) and entirely change the model behavior and resulting error signal.

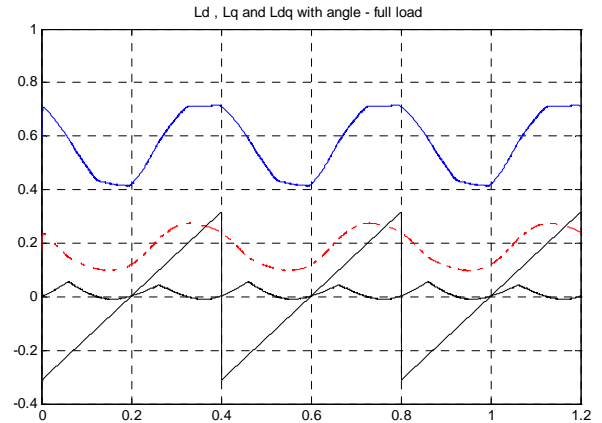


Fig. 9. Trajectories of L_d , L_q and L_{dq} inductances for full circle of rotor position errors and maximum current.

IV. EXPERIMENTAL RESULTS

The proposed IPMSM model was verified by using an experimental setup consisting vector controlled 1kW IPMSM machine, Fig. 10. The IPMSM parameters are – rated power $P_n = 750W$, with 36.5 V_{L-L} peak BEMF at 1000 rpm, star connected stator, $P = 4$, $R_s = 3.8\Omega$, and inductance parameters as given in figures 1, 2 and 4.

Motor was kept at stand still with lock rotor bracket. The magnet and encoder position was preset to zero. HF test

signal, amplitude 0.2 A and frequency 250 Hz, was injected in slowly rotating estimated rotor position, DSP d-axis. Shown demodulated rotor position error signal is calculated using model at Figure 5. The data from DSP was transferred into PC via fast GUI interface.



Fig.10. Experimental setup.

Fig. 11. shows the demodulated error signal relatively to sawtooth estimated position signal. With real magnet position kept at zero that sawtooth is also position error signal. Dashed red line shows data collected for zero current condition $I_d=0A$, $I_q=0A$ and shows very close match to both IPMSM models. Solid blue line for full load condition ($I_d = -4.5A$, $I_q = 5.5A$) shows complex nature of demodulated error signal. While original IPMSM model show no change with load (Fig 7.) modified IPMSM model (Fig 8.) shows similar output HF error distortion.

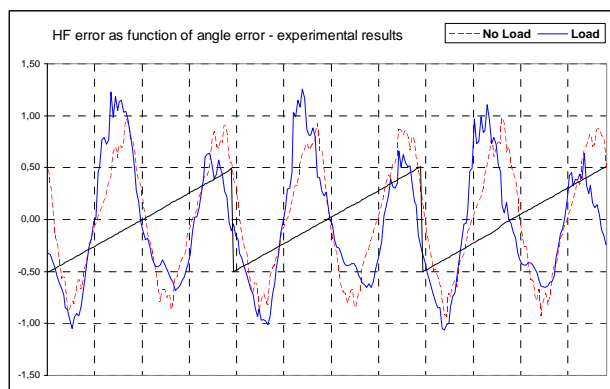


Fig. 11. Demodulated HF error signal as function of rotor position error for no load (dashed) and full load (solid) –experimental results.

V. CONCLUSION

This paper describes a modified IPMSM model that includes all known saturation effects. The motivation for this

model development was HF test signal based sensorless instability at ultra high load condition. The modified IPMSM model results suggest the reason for that unwanted sensorless behavior. It shows large distortion of demodulated position error signal which can lead to 1. significant estimated position error (the zero crossing of error signal and actual zero position error differ) or 2. regulator instability, especially if error signal offsets from zero and loses zero-crossing. In that case regulator runs through actual zero position and runs to next available zero crossing where it settles erroneously.

REFERENCES

- [1] Angus Murray, Marco Palma and Ali Husain, "Performance Comparison of Permanent Magnet Synchronous Motors and Controlled Induction Motors in Washing Machine Applications using Sensorless Field Oriented Control", Energy Saving Products Division International Rectifier El Segundo, CA 90245.
- [2] Y.-S. Jeong, R. D. Lorenz, T. M. Jahns and S.-K. Sul, "Initial Rotor Position Estimation of an Interior Permanent Magnet Synchronous Machine using Carrier-Frequency Injection Methods," IEEE Intern. Electric Machines and Drives Conf. IEMDC, Madison, WI, June 1-4, 2003, pp. 1218–1223; later in IEEE Trans. Industry Appl., Vol. 41, No. 1, Jan./Feb. 2005, pp. 38-45.
- [3] M. J. Corley and R. D. Lorenz, "Rotor position and velocity estimation for a salient-pole permanent magnet synchronous machine at standstill and high speed," IEEE Trans. Ind. Appl., vol. 34, no. 4, pp. 784–789, Jul./Aug. 1998.
- [4] G. Foo and M. F. Rahman, "Sensorless sliding-mode MTPA control of an IPM synchronous motor drive using a sliding-mode observer and HF signal injection," IEEE Trans. Ind. Electron., vol. 57, no. 4, pp. 1270–1278, Apr. 2010.
- [5] Chan-Hee Choi and Jul-Ki Seok, "Pulsating Signal Injection-Based Axis Switching Sensorless Control of PMSM for Minimal Zero Current Clamping Effects", School of Electrical Engineering, Yeungnam University DaeDong, Kyungsan, Kyunbuk, Korea (ZIP : 712-749)
- [6] Y. Li, Z. Q. Zhu, D. Howe, and C. M. Bingham, "Modeling of Cross-Coupling Magnetic Saturation in Signal-Injection-Based Sensorless Control of Permanent-Magnet Brushless AC Motors", IEEE Transactions on Magnetics, vol. 43, no. 6, June 2007.
- [7] H. W. De Kock, M. J. Kamper, and R. M. Kennel, "Anisotropy comparison of reluctance and PM synchronous machines for position sensorless control using HF carrier injection," IEEE Trans. Power Electron., vol. 24, no. 8, pp. 1905–1913, Aug. 2009.
- [8] P. Guglielmi, M. Pastorelli, and A. Vagati, "Impact of cross-saturation in sensorless control of transverse-laminated synchronous reluctance motors," IEEE Trans. Ind. Electron., vol. 53, no. 2, pp. 429–439, Apr. 2006.
- [9] N. Bianchi and S. Bolognani, "Influence of rotor geometry of an interior PM motor on sensorless control feasibility," IEEE Trans. Ind. Appl., vol. 43, no. 1, pp. 87–96, Jan./Feb. 2007.
- [10] Y. Li, Z. Q. Zhu, D. Howe, C.M. Bingham, and D. Stone, "Improved rotor position estimation by signal injection in brushless AC motors, accounting for cross-coupling magnetic saturation," IEEE Trans. Ind. Appl., vol. 45, no. 5, pp. 1843–1849, Sep./Oct. 2009.